

A New Convolutional Neural Network-Based Data-Driven Fault Diagnosis Method

Long Wen^{1b}, Xinyu Li^{1b}, Liang Gao^{1b}, *Member, IEEE*, and Yuyan Zhang^{1b}

Abstract—Fault diagnosis is vital in manufacturing system, since early detections on the emerging problem can save invaluable time and cost. With the development of smart manufacturing, the data-driven fault diagnosis becomes a hot topic. However, the **traditional data-driven fault diagnosis methods rely on the features extracted by experts**. The feature extraction process is an exhausted work and greatly impacts the final result. Deep learning (DL) provides an effective way to extract the features of raw data automatically. Convolutional neural network (CNN) is an effective DL method. In this study, a new CNN based on LeNet-5 is proposed for fault diagnosis. Through a conversion method **converting signals into two-dimensional (2-D) images**, the proposed method can extract the features of the converted 2-D images and eliminate the effect of handcrafted features. The proposed method which is tested on three famous datasets, including motor bearing dataset, self-priming centrifugal pump dataset, and axial piston hydraulic pump dataset, has achieved prediction accuracy of 99.79%, 99.481%, and 100%, respectively. The results have been compared with other DL and traditional methods, including adaptive deep CNN, sparse filter, deep belief network, and support vector machine. The comparisons show that the proposed CNN-based data-driven fault diagnosis method has achieved significant improvements.

Index Terms—Convolutional neural network (CNN), data-driven, fault diagnosis, image classification.

I. INTRODUCTION

FAULT diagnosis has attracted many studies in the recent years [1], [2]. Early detections on the emerging problem are vital for the complex systems, and it can save invaluable time and cost to take remedy measure to avoid dangerous situations. In general, the fault diagnosis methods can be classified into model-based, signal-based, knowledge-based, and hybrid/active

methods [3]. The knowledge-based methods, which are also named as data-driven methods, require a large volume of historic data to establish the fault modes about the systems without priori known models or signal patterns. They are very suitable for the complex systems which are difficult to establish the explicit models or signal symptoms. Recently the smart manufacturing is boosting, and the data in enterprise can be collected much faster [4] and more widely than ever before. This provides new opportunities for the data-driven fault diagnosis methods to make full use of the massive mechanical data [5], and has received more and more attentions from the researchers and engineers.

Machine learning is one of the main methods to handle the data in data-driven fault diagnosis. The initial attempts of applying support vector machines (SVMs) to fault diagnosis were in the late 1990s [6]. Fuzzy logic (FL) can partition the feature space into fuzzy sets and utilize fuzzy rules for reasoning. A novel fuzzy-neural data fusion engine was proposed to the on-line monitoring and diagnosis [7]. Artificial neural network (ANN) is one of the most well-established data-driven fault diagnosis methods. An extension neural network was applied on the fault diagnosis in internal combustion engines [8]. A feedforward neural network was applied on the laser welding process monitoring and defects diagnosis [9]. However, machine learning methods are unable to generate discriminative features of raw data and are always combined with the signal features extraction process. This features extraction process is an exhausted work and greatly impacts the final result.

With the rapid development of machine learning, deep learning (DL) has emerged as an effective way to overcome the above drawback. DL can learn the abstract representation features [10] of the raw data automatically [11], which could avoid the handcrafted features designed by engineers. Several DL methods had already been applied on the fault diagnosis, such as deep belief network (DBN) [12], sparse auto-encoder [13], stacked denoising auto-encoder [14], [15], and sparse filtering [16]. DL has achieved the good results compared with the traditional shadow machine learning methods, but the application of DL on fault diagnosis is still developing.

As one of the most effective DLs, convolutional neural network (CNN) has also been applied on the fault diagnosis. Since the most common data type is the time-domain signals, the one-dimensional (1-D) CNN has been investigated on the real-time motor fault diagnosis [17]. In some scenarios, the machinery data can be presented in 2-D format (such as time-frequency spectrum), and then an image processing method is combined to classify these images [18]. However, these

Manuscript received June 22, 2017; revised September 3, 2017 and October 6, 2017; accepted October 28, 2017. Date of publication November 17, 2017; date of current version March 6, 2018. This work was supported in part by the Natural Science Foundation of China (NSFC) under Grant 51435009, Grant 51775216, and Grant 51711530038, in part by the China Postdoctoral Science Foundation under Grant 2017M622414, and in part by the 111 Project under Grant B16019. (Corresponding author: Liang Gao.)

The authors are with the Department of Industrial and Manufacturing Systems Engineering, State Key Laboratory of Digital Manufacturing Equipment and Technology, School of Mechanical Science and Engineering, Huazhong University of Science and Technology, Wuhan 430074, China (e-mail: wenlong@hust.edu.cn; lixinyu@hust.edu.cn; gaoliang@mail.hust.edu.cn; 419661350@qq.com).

Color versions of one or more of the figures in this paper are available online at <http://ieeexplore.ieee.org>.

Digital Object Identifier 10.1109/TIE.2017.2774777

presentations rely on the expert's knowledge as well. In this study, a new data preprocessing method is introduced to convert the raw time-domain signal data into the 2-D gray images without any predefined parameters, which can eliminate the experts' experiences as more as possible. Then, a new improved CNN is proposed to extract the features of these 2-D images. The results show that it is very promoting in fault diagnosis.

The main contributions of this paper are summarized as the following three points. First, a new data preprocessing method named as a signal-to-image conversion method is developed to extract the 2-D features of raw data without predefined parameters. Second, an improved CNN is proposed by using a deeper structure and the zero-padding method to increase the nonlinearity of the features. Third, as a result, the proposed CNN-based fault diagnosis method achieves a significant improvement by comparing with other DL and traditional methods.

The rest of this paper is organized as follows. Section II discusses the related works. Section III presents the methodologies, including the signal-to-image conversion method and the proposed CNN method. Section IV presents the testing results of the proposed method on three datasets. The conclusion and future research works are presented in the Section V.

II. RELATED WORKS

The related works described in this section contain the data-driven fault diagnosis method and LeNet-5 CNN.

A. Data-Driven Fault Diagnosis Methods

Since the data-driven fault diagnosis methods can discover the underlying knowledge to represent the information among the system variables only using historic data, it is very suitable for the complex systems where they are difficult to establish the explicit models or signal symptoms. The first data-driven fault diagnosis was published in 1980s using the expert system [19]. With the rapid development of machine learning and smart manufacturing, the data-driven fault diagnosis method has become a hot research topic recently.

The intelligent learning from the large volume of historic data is essential for the data-driven fault diagnosis method. The statistical analysis methods, including principal component analysis (PCA), partial least squares (PLS), and independent component correlation, have received considerably increasing attentions for industrial process monitoring [20]. Yin *et al.* [21] investigated the data-driven process monitoring based on a modified PLS. Yin *et al.* [22] studied a data-driven real-time implementation of fault-tolerant control system. Machine learning is also one of the dominant tools for data-driven fault diagnosis, such as SVM [6], FL [7], ANN [8], etc. Further, the statistical and machine learning methods are often utilized jointly. Grbovic *et al.* [23] investigated cold start fault detection framework, in which only normal operating data were available at the beginning and the fault can be observed by the PCA with squared prediction error statistics.

Compared with the traditional artificial intelligent techniques, DL holds the potential of feature representation and has been applied in the machine health monitoring field [24]. The key aspect of DL is that these features are not designed by human engineers,

which can reduce the impacts of different experiences coming from different engineers. Jia *et al.* [25] investigated a deep neural network for intelligent fault diagnosis based on auto-encoder. Liao *et al.* [26] studied the enhanced restricted Boltzmann machine for prognostics and health assessment. Gan and Wang [27] applied a DBN-based hierarchical diagnosis network (HDN) on the fault diagnosis of rolling element bearings. Cho *et al.* [28] investigated recurrent neural networks and dynamic Bayesian modeling on the induction motors fault detection.

As one of the most effective DL method, CNN has also been applied on the fault diagnosis. Ince *et al.* [17] applied 1-D CNN to real-time motor fault diagnosis. Abdeljaber *et al.* [29] studied 1-D CNN to real-time damage detection. Guo *et al.* [30] investigated a hierarchical adaptive deep CNN to bearing fault diagnosis.

In some scenarios, the machinery data can be presented in 2-D format. The conversion from 1-D raw signals to 2-D images is various. Chong [31] proposed an approach to effectively extract features of the faults in an induction motor. He converted 1-D vibration signals into 2-D gray-level images. Kang and Kim [32] proposed a 2-D grey images representation based on Shannon wavelets and applied multiclass SVMs for identifying faults in the induction machine. Li *et al.* [33] investigated a feature-extraction model based on 2-D nonnegative matrix factorization and generalized S transform proposed. Lu *et al.* [18] proposed a conversion from signals to images using bispectrum, and then used a probabilistic neural network to classify the images. However, most of these conversions rely on expert's knowledge as well. In this study, a new signal-to-image conversion method is presented without any predefined parameters, which can eliminate the experts' experiences as more as possible.

B. LeNet-5 CNN

CNN is a special structure of ANN. Different from the fully connected (FC) ANN, each neuron of the feature map in each layer is only sparsely connected to a small set of neurons in previous layer in CNN. This was inspired by the concept of simple and complex cells in visual cortex in brain [34], and the visual cortex contains some cells that are only sensitive to the local receptive field [35].

There are three major layers in CNN: 1) convolutional layer; 2) pooling layer; and 3) FC layer. The convolutional layer applies a set number of filters to obtain the feature maps of input images. The pooling layer is the down-sampling layer to reduce the feature dimensions of the input. After several alternating convolutional and pooling layers, the FC layers are followed to compute the class scores. CNN has achieved widely successful applications in image recognition tasks. And there are some famous CNN models, such as LeNet-5 [36], AlexNet [37], VGGNet [38], GoogLeNet [39], etc.

LeNet-5, which is a classical release of CNN, has been applied to handwritten and machine-printed character recognition with minimal data preprocessing. There are two alternating convolutional and pooling layers in this model, with a two-layer FC ANN. Hong *et al.* [40] employed a LeNet-5 to face recognition. Ren *et al.* [41] used PCA-based CNN for the image

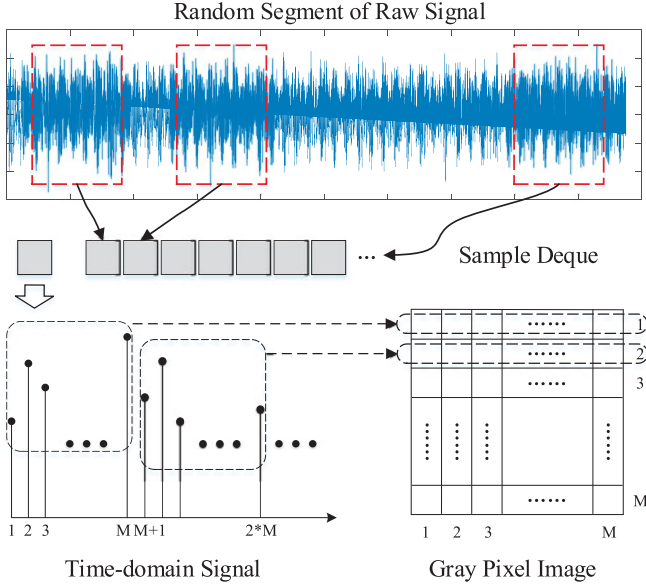


Fig. 1. Signal-to-image conversion method.

classification task. Guo *et al* [30] investigated the LeNet-5-based adaptive deep CNN on the bearing fault diagnosis.

In this study, the CNN models based on LeNet-5 are designed to solve the image classification tasks of the fault diagnosis.

III. PROPOSED CNN FOR FAULT DIAGNOSIS

This section presents the proposed CNN-based fault diagnosis method. First, the signal-to-image conversion method is presented to handle the raw signal. Then, the modified CNN is presented. Moreover, the zero-padding method is also introduced.

A. Signal-to-Image Conversion Method

In traditional data-driven fault diagnosis methods, the data preprocessing method is vital since most of the data-driven methods cannot handle the raw signals directly. One of the main functions of the data preprocessing method is to extract the features of the raw signals from the large volume of historic data. However, to extract the proper features is an exhausted work, and these features have great effects on the final results. In this study, an effective data preprocessing method is developed. The idea of this method is to convert the time-domain raw signals into images.

As shown in Fig. 1, in this conversion method, the time-domain raw signals fulfill the pixels of the image by sequence. In order to obtain an $M \times M$ size image, a segment signal with the length M^2 would be randomly obtained from the raw signal. Let $L(i)$, $i = 1, \dots, M^2$, denotes the value of the segment signal. $P(j, k)$, $j = 1, \dots, M$, $k = 1, \dots, M$ denotes the pixel strength of the image, as shown in the following equation:

$$P(j, k) = \text{round} \left\{ \frac{L((j-1) \times M + k) - \text{Min}(L)}{\text{Max}(L) - \text{Min}(L)} \times 255 \right\}. \quad (1)$$

The function $\text{round}(\cdot)$ is the rounding function and the whole pixel value has been normalized from 0 to 255, which is just the pixel strength of the gray image. The 2×2 filters are commonly used in this paper, and the size of image features on each layer would be reduced by half, so the recommendation of M is 2^n , such as 16, 32, 64, 128, etc. In this paper, the selection of 64×64 and 16×16 is depended on the volume of signal data.

The advantage of this data processing method is that it provides a way to explore 2-D features of the raw signals [31]. What's more, this data preprocessing method can be calculated without any predefined parameters and can reduce the experts' experiences as more as possible.

B. Proposed CNN Structure

Once the raw signals have been converted to images, a CNN can be trained to classify these images. LeNet-5 which is a classical CNN is effective and promoting in the image pattern recognition. In this study, the CNN models based on LeNet-5 are designed to solve the image classification tasks of the fault diagnosis.

The sizes of images in LeNet-5 are 32×32 . But in order to improve the classification results, the sizes of images change according to the volume of signals data in this study. In the first and second cases, the signals data have the large volumes, and larger images size can promote the classification result. So the sizes of images in these cases are 64×64 . Oppositely, since the volume of signals data is relatively small in the third case, the sizes of images are 16×16 .

In the proposed CNN models, they contain four alternating convolutional and pooling layers with one or two FC layers for 64×64 images. While the proposed CNN models only contain two alternating convolutional and pooling layers with one FC layers for 16×16 images. The padding method is also different from original LeNet-5, and the zero padding is used in our study. Fig. 2 shows the basic structure of the proposed CNN models for 64×64 images.

C. Zero-Padding Method

Padding method is an important technique to control the size of feature dimension. The zero-padding method is applied on the CNN models to prevent the dimension loss, which is shown in Fig. 3. Let M be the input size, N be the output size, F be the filter width, and S be the stride. The number of padding on left PL and on right PR can be calculated by the following equations.

$$N = \text{ceil} \left(\frac{M}{S} \right) \quad (2)$$

$$PT = (N - 1) \times S + F - M \quad (3)$$

$$PL = \text{floor} \left(\frac{PT}{2} \right) \quad (4)$$

$$PR = PT - PL \quad (5)$$

where $\text{ceil}(\cdot)$ and $\text{floor}(\cdot)$ are the ceil and floor functions, respectively.

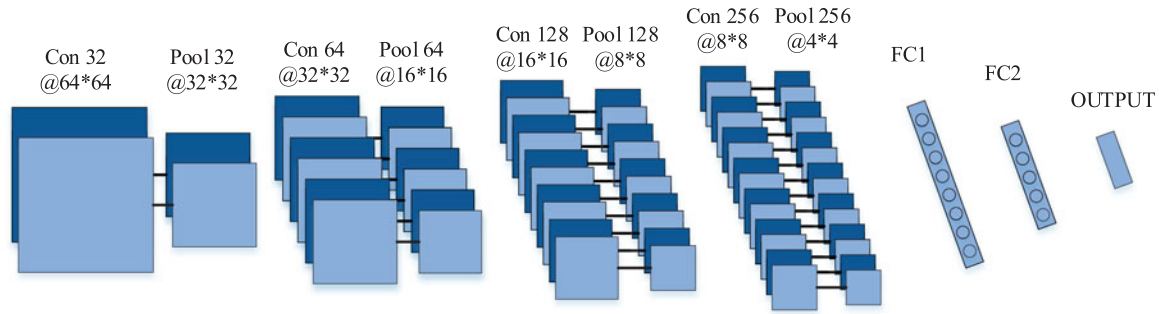


Fig. 2. Proposed CNN structure for 64×64 images.

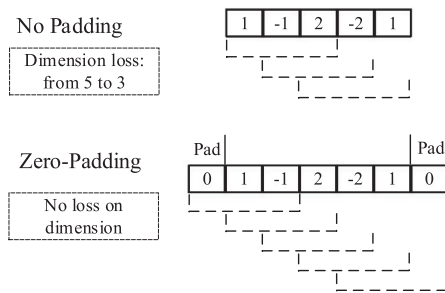


Fig. 3. Zero-padding method used in CNN.

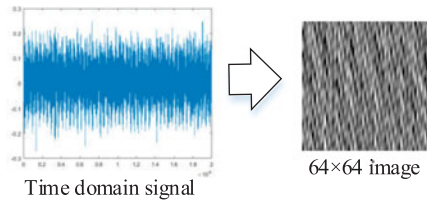


Fig. 4. Signal-to-image conversion image on normal condition.

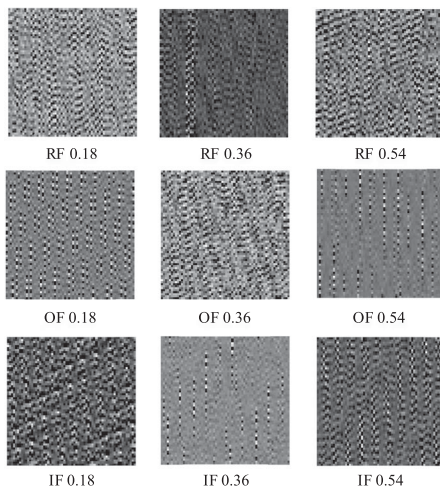


Fig. 5. Converted images on nine fault conditions.

In the zero-padding method, zeros would be added automatically to fill the convolution process. Fig. 3 shows an example of zero-padding method in one dimension. The parameters are $M = 5$, $S = 1$, $F = 3$, then the padding result will be

TABLE I
LAYER CONFIGURATIONS OF CNN MODELS

| Layer name | CNN Models |
|------------|---------------------------------|
| L1 | Conv($5 \times 5 \times 32$) |
| L2 | Maxpool(2×2) |
| L3 | Conv($3 \times 3 \times 64$) |
| L4 | Maxpool(2×2) |
| L5 | Conv($3 \times 3 \times 128$) |
| L6 | Maxpool(2×2) |
| L7 | Conv($3 \times 3 \times 256$) |
| L8 | Maxpool(2×2) |

TABLE II
RESULT OF CNN MODELS WITH ONE FC LAYER IN CASE 1 (%)

| No. | CNN-1024 | CNN-1536 | CNN-2048 | CNN-2560 | CNN-3072 | CNN-3584 |
|------|----------|----------|----------|---------------|----------|----------|
| Max | 99.78 | 99.83 | 99.87 | 99.85 | 99.74 | 99.86 |
| Min | 99.11 | 99.59 | 99.57 | 99.67 | 99.41 | 98.811 |
| Mean | 99.57 | 99.71 | 99.75 | 99.77 | 99.65 | 99.63 |
| Std | 0.2063 | 0.0658 | 0.0779 | 0.0544 | 0.0979 | 0.3548 |

$PL = 1$, $PR = 1$, $N = 5$. It should be noted that the strides of the convolutional and pooling layers are set to 1 in this study.

IV. CASE STUDIES AND EXPERIMENTAL RESULTS

In this section, the proposed CNN-based fault diagnosis method is conducted on three famous fault diagnosis datasets, which are the motor bearing fault dataset, the self-priming centrifugal pump dataset, and the axial piston hydraulic pump dataset. The CNN models are written in Python 3.5 with TensorFlow and run on Ubuntu 16.04 with a GTX 1080 GPU.

A. Case 1: Motor Bearing Fault Diagnosis

In this section, the proposed CNN-based method is conducted on the famous motor bearing data provided by the Case Western Reserve University [42]. In this dataset, there are three fault types, and each fault type has three different damage sizes. There are totally ten health conditions with nine fault conditions and one normal condition (NO). Three fault types are roller fault (RF), outer race fault (OF), and inner race fault (IF). The damage sizes are the 0.18, 0.36, and 0.54 mm.

TABLE III
RESULT OF CNN MODELS WITH TWO FC LAYERS IN CASE 1 (%)

| No. | CNN-2560 | CNN-2560-64 | CNN-2560-128 | CNN-2560-256 | CNN-2560-512 | CNN-2560-768 | CNN-2560-1024 |
|------|----------|-------------|--------------|--------------|--------------|---------------------|---------------|
| Max | 99.85 | 99.87 | 99.89 | 99.88 | 99.84 | 99.91 | 99.88 |
| Min | 99.67 | 99.66 | 99.55 | 99.70 | 99.69 | 99.70 | 99.44 |
| Mean | 99.77 | 99.75 | 99.76 | 99.78 | 99.78 | 99.79 | 99.77 |
| Std | 0.0544 | 0.0725 | 0.0984 | 0.0526 | 0.0476 | 0.0759 | 0.1275 |

The driven end vibration signals are collected under four load conditions (0, 1, 2, 3 hp) to verify the performance of the proposed method. There are 2000 samples per load condition in the training dataset and 400 samples per load condition in the testing dataset. All the samples are randomly selected from the dataset. It should be noticed that the sampling without replacement is used, so the samples in the training dataset and testing dataset are totally different.

1) Image Conversion Result: The size of the converted images is set as 64×64 . The signal conversion result on normal condition is presented in Fig. 4. The converted gray image contains 4096 pixels. The conversion results on other nine fault conditions are presented in Fig. 5. From the converted images, it can be observed that the **images of different fault conditions look totally different from each other, and this provides an intuitionistic way to classify them.**

2) CNN Structure Testing Result: The CNN structure on this case study contains four alternating convolutional and pooling layers with one or two FC layers. The parameters on each layer are presented in Table I. FC1 is the first FC layer, and FC2 is the second FC layer. The denotation of Conv($5 \times 5 \times 32$) means that it is a convolution layer, and the filter size is 5×5 with 32 channels. Maxpool(2×2) means that it is a maxpool layer with 2×2 filters. The results of the proposed CNN models with one FC layer are presented in Table II, and those of the proposed CNN models with two FC layers are presented in Table III.

CNN- i - j denotes that there are i neurons in FC1 and j neurons in FC2, such as CNN-2560 means there are 2560 neurons in FC1, and the FC2 layer does not exist. All CNN models run ten times, and the maximum, minimum, mean, and the standard deviation of the prediction accuracy are the results measure terms.

There are six CNN models with one FC layer. From the results, CNN-2560 achieves the best result. Its mean accuracy is 99.77%, the minimum accuracy is 99.67%, and the standard deviation is 0.0544. The best maximum accuracy is CNN-2048, which is 99.87% and slightly superior than CNN-2560, whose maximum is 99.85%. The prediction results of these CNN like an “inverted U” type, showing that CNN-2560 is the peak of this proposed CNN models.

The CNN models with two FC layers are based on CNN-2560. There are six CNN models. From the results, it can be seen that all these CNN models are very close to each other. CNN-2560-64, CNN-2560-128, and CNN-2560-1024 are slightly inferior to CNN-2560. CNN-2560-256, CNN2560-523, and CNN-2560-

TABLE IV
COMPARISON RESULT OF CNN MODELS AND OTHER METHODS (%)

| Methods | Mean Accuracy |
|---------------|---------------|
| CNN | 99.79 |
| Sparse filter | 99.66 |
| ADCNN | 98.1% |
| DBN | 87.45 |
| DBN Based HDN | 99.03 |
| SVM | 87.45 |
| ANN | 67.70 |

768 improve the prediction accuracy slightly. The best among these CNN models is CNN-2560-768, and its mean accuracy is 99.79%, the maximum accuracy is 99.91%, and the minimum accuracy is 99.70%.

3) Compared With Other Methods: In order to evaluate the performances of the proposed CNN models, other statistical methods and DL methods are selected to compare the prediction accuracy in this case. They are sparse filter [16], DBN [12], DBN-based HDN [27], SVM [43], ANN [12], and adaptive deep convolution neural network (ADCNN) [30]. The mean prediction accuracy is the final measure term for this comparison. The comparison results are shown in Table IV, and CNN stands for the CNN-2560-768.

From the results, it can be seen that the proposed CNN method obtains a wonderful result compared with these methods. The mean prediction accuracy is as high as 99.79%, and it is better than all other methods. The prediction results of sparse filter, DBN, DBN-based HDN, SVM are 99.66%, 87.45%, 99.03%, and 87.45%, respectively, which shows the significant performance of the proposed CNN method. The result of traditional ANN is 67.7%, which is obviously inferior to the proposed CNN models, showing the great improvement of the proposed CNN method.

Fig. 6 presents the confusion matrix of the best result of CNN-2560-768, which obtains the prediction accuracy of 99.91% (the maximum value of CNN-2560-768 in Table III). The rows stand for the actual label, and the columns stand for the predicted label for each condition. It shows that OF0.18, OF0.36, IF0.18, IF0.54, and NO have 100% accuracy. RF0.54 is the worst one which has the accuracy of 99.63%. RF0.36 receives the most misclassification. 0.19% out of RF0.54, 0.06% out of OF0.54 and IF0.36 are misclassified to RF0.36. OF0.18 and NO have 100% accuracy, what's more, no other condition is misclassified to them, meaning they are purely separated from other conditions.

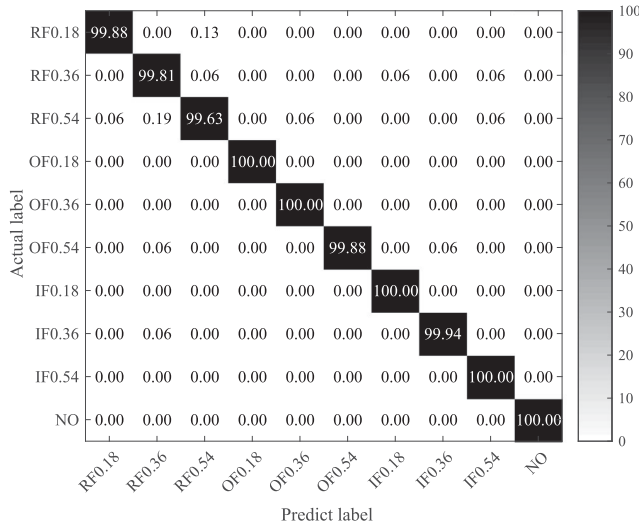


Fig. 6. Confusion matrix of the result on CNN-2056-768.

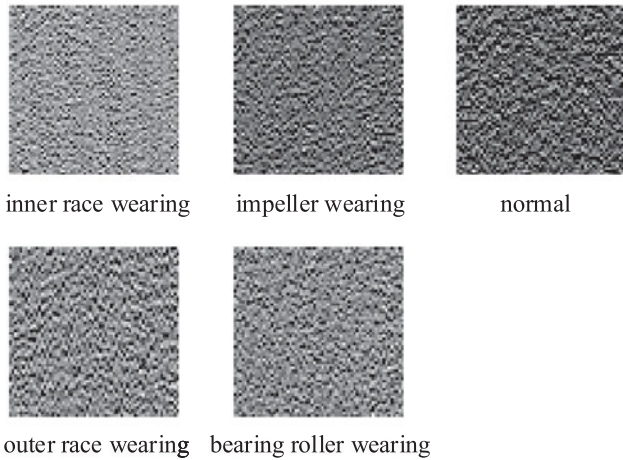


Fig. 7. Converted images in case 2.

B. Case 2: Self-Priming Centrifugal Pump Fault Diagnosis

In this section, the proposed method is conducted on self-priming centrifugal pump [18]. The acceleration sensor is installed on a specific pedestal above the motor housing. In the data acquisition system, the rotation speed is 2900 per minute. The sampling frequency of vibration signals is 10 240 Hz. There are four faults conditions and one normal condition (NO). The fault conditions are bearing roller wearing (BR), inner race wearing (IR), outer race wearing (OR), and impeller wearing (IW) fault condition.

1) Image Conversion Result: In this case, the sampling time is 2 s for each dataset, and each condition is collected five times. The size of the converted images is 64×64 , and they are presented in Fig. 7. The samples in the training dataset and the testing dataset are 2000 and 400 per conditions. There are totally 50 000 images in the training dataset and 10 000 images in the testing dataset.

TABLE V
RESULT OF CNN MODELS WITH ONE FC LAYER IN CASE 2 (%)

| No. | CNN-512 | CNN-1024 | CNN-1536 | CNN-2048 | CNN-2560 | CNN-3072 |
|------|---------|----------|---------------|----------|----------|----------|
| Max | 99.40 | 99.48 | 99.67 | 99.68 | 99.65 | 99.55 |
| Min | 97.60 | 99.18 | 99.12 | 98.55 | 99.03 | 99.21 |
| Mean | 98.915 | 99.322 | 99.445 | 99.411 | 99.397 | 99.379 |
| Std | 0.5266 | 0.1140 | 0.1850 | 0.3380 | 0.2134 | 0.1034 |

TABLE VI
RESULT OF CNN MODELS WITH TWO FC LAYERS IN CASE 2 (%)

| No. | CNN-1536 | CNN-1536-32 | CNN-1536-64 | CNN-1536-128 | CNN-1536-256 | CNN-1536-512 |
|------|----------|-------------|-------------|---------------|--------------|--------------|
| Max | 99.67 | 99.74 | 99.69 | 99.74 | 99.63 | 99.56 |
| Min | 99.12 | 98.95 | 99.24 | 99.11 | 99.20 | 99.25 |
| Mean | 99.445 | 99.35 | 99.472 | 99.481 | 99.397 | 99.401 |
| Std | 0.1850 | 0.2621 | 0.1677 | 0.1966 | 0.1528 | 0.1106 |

TABLE VII
COMPARISON RESULT OF CNN AND SURF-BASED PNN IN CASE 2 (%)

| | CNN-1536-128 | SURF-based PNN | | | |
|------|---------------|----------------|--------|--------|--------|
| | | Test 1 | Test 2 | Test 3 | Test 4 |
| Max | 99.74 | 99.11 | 100 | 96.00 | 98.22 |
| Mean | 99.481 | | 98.33 | | |
| Std | 0.1966 | | 1.7164 | | |

2) CNN Structure Testing Result: The basic structure of CNN in this case study is the same with case 1 in Section IV-A, except that they have different neurons on FC layers. There are six CNN models with one FC layer and five CNN models with two FC layers. In the comparison, all CNN models run ten times. In Table V, it can be seen that CNN-1536 achieves the best mean accuracy which is 99.445%. The result of CNN-2048 is slightly inferior to CNN-1536, and the mean accuracy is 99.411%.

Table VI presents the result of CNN model with two FC layers. These five CNN models are based on CNN-1536. Among these CNN models, CNN-1536-64 and CNN-1536-128 are better than CNN-1536 and the accuracy of CNN-1536-128 is 99.481% with the standard deviation of 0.1966.

3) Compared With Other Methods: The results of the proposed CNN models are compared with the method in literature [18], and they are presented on Table VII. The speeded up robust features (SURF)-based PNN employs bispectrum technique to transform the vibration signals into images, and uses SURF-based PNN to classify the fault diagnosis. From the results, it can be clearly seen that the proposed CNN method outperforms SURF-based PNN in terms of the mean accuracy and the standard deviation of the accuracy, showing the potential of the proposed CNN-based fault diagnosis method.

The confusion matrix of the best result of CNN-1536-128 is presented on Fig. 8 (the maximum value of CNN-1536-128 in

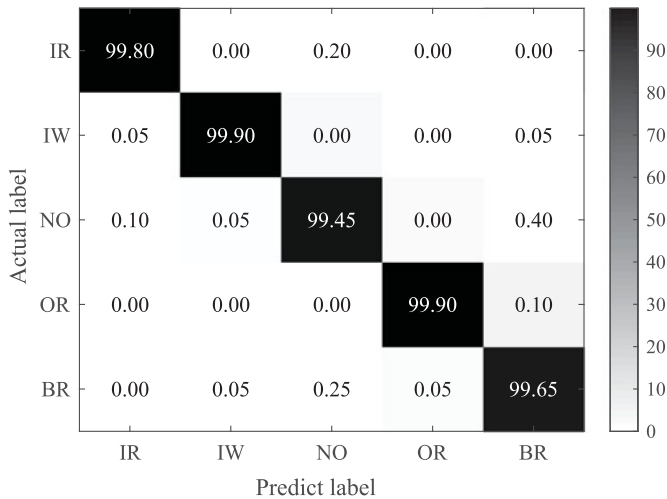


Fig. 8. Confusion matrix of the result on C1536-128.

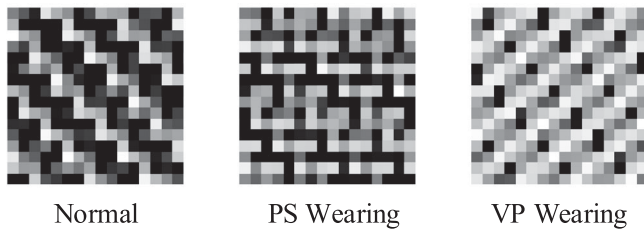


Fig. 9. Converted images in case 3.

Table VI). From the result, the normal condition has the worst accuracy of 99.45%, and IW wearing and OR wearing have the accuracy of 99.90%. The most misclassification is 0.4%, where the actual label is normal condition but the prediction label is BR wearing.

C. Case Study 3: Axial Piston Hydraulic Pump Fault Diagnosis

In this section, the proposed method is tested on the axial piston hydraulic pump [18]. In the experiment, the rotation speed is 5280 r/min, and the corresponding spindle frequency is 88 Hz. The accelerograph is installed at the end face of the pump, and the sampling frequency is 1 kHz. There are two fault conditions in this case. They are the piston shoes and swashplate wearing (PS wearing) and valve plate wearing (VP wearing). The normal condition is also collected as contrast.

1) Image Conversion Result: In this case, each running condition contains only 1024 points, which is relatively small compared with the above two datasets. So the size of images is 16×16 , and the converted images are presented in Fig. 9. The samples in the training dataset and the testing dataset are 400 and 100 per condition. The structure of CNN contains two convolutional layers and max-pool layers. The channels of these two convolutional layers are 16 and 64. The filter size of convolution is 3×3 , and that of maxpool is 2×2 .

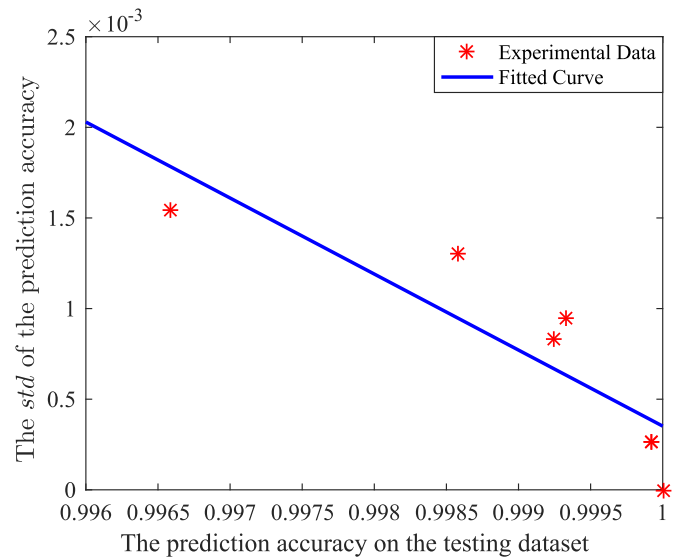


Fig. 10. Fitted curve of prediction accuracies and its standard deviation.

2) CNN Structure Testing Result: The results of the proposed methods are presented in Table VIII. Seven CNN models are tested and each CNN model runs ten times. CNN-0 means that there does not exist the FC layer.

3) Compared With Other Methods: The prediction accuracy on testing dataset of CNN-8 is 100% in Table VIII. This result outperforms all other CNN models. The mean prediction accuracy decreases obviously with the increase of the number of neurons in FC layer. What's more, the prediction accuracy (a) and its standard deviation (std) show a strong linear relationship. The multiple correlation coefficient R^2 is 0.7686, and the linear regressive function is: $\text{std} = 0.4198 - 0.4195a$. The fitted curve is plotted in Fig. 10.

The results are also compared with the literature [18], and the result is presented in Table IX. From the result, it can be clearly seen that the proposed CNN method outperforms SURF-based PNN. Even though PNN has achieved a good result on the prediction accuracy of 98.705%. The proposed CNN-based model achieves a stable prediction of 100%. This result validates the performance of the proposed CNN method.

D. Discussions

In the case studies, the potential of the proposed CNN-based fault diagnosis method is validated on three datasets (the famous motor bearing dataset, self-priming centrifugal pump dataset, and axial piston hydraulic pump dataset). According to the volumes of the signals, the sizes of converted images are 64×64 , 64×64 , and 16×16 . The prediction accuracies of the proposed CNN are 99.79%, 99.481%, and 100% on these three datasets, respectively. Since the proposed method can extract the 2-D features of the converted images automatically, these results outperform other DL and traditional methods, such as ADCNN, sparse filter, DBN, SVM, ANN, and SURF-based PNN, which shows the potential of the proposed method.

TABLE VIII
RESULT OF DIFFERENT CNN MODELS IN CASE 3 (%)

| Run No. | CNN-0 | CNN-8 | CNN-16 | CNN-32 | CNN-64 | CNN-128 | CNN-256 |
|---------|--------|------------|--------|--------|--------|---------|---------|
| 1 | 99.50 | 100 | 100 | 100 | 100 | 99.83 | 99.92 |
| 2 | 99.50 | 100 | 99.92 | 100 | 99.83 | 99.91 | 99.92 |
| 3 | 99.50 | 100 | 100 | 100 | 100 | 100 | 99.58 |
| 4 | 99.67 | 100 | 100 | 100 | 99.75 | 99.91 | 99.92 |
| 5 | 99.75 | 100 | 100 | 100 | 99.83 | 99.91 | 100 |
| 6 | 99.50 | 100 | 100 | 100 | 100 | 100 | 99.92 |
| 7 | 99.75 | 100 | 100 | 99.92 | 100 | 100 | 99.75 |
| 8 | 99.83 | 100 | 100 | 100 | 100 | 99.75 | 99.75 |
| 9 | 99.67 | 100 | 100 | 100 | 100 | 100 | 100 |
| 10 | 99.92 | 100 | 100 | 100 | 99.92 | 99.92 | 99.83 |
| Mean | 99.66 | 100 | 99.99 | 99.99 | 99.93 | 99.93 | 99.86 |
| Std | 0.1544 | 0 | 0.0263 | 0.0263 | 0.0946 | 0.0829 | 0.1306 |

TABLE IX
COMPARISON RESULT OF CNN AND SURF-BASED PNN IN CASE 3 (%)

| | CNN-8 | SURF-based PNN | | | |
|------|------------|----------------|-----|--------|-------|
| | | 1 | 2 | 3 | 4 |
| Max | 100 | 97.04 | 100 | 100 | 97.78 |
| Mean | 100 | | | 98.705 | |
| Std | 0 | | | 1.5255 | |

V. CONCLUSION AND FUTURE RESEARCH WORKS

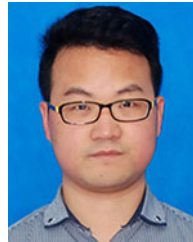
This study presented a new CNN-based fault diagnosis method. The main contributions of this study are developing a signal-to-image conversion method, proposing a new CNN based on LeNet-5, and applying the CNN models to the fault diagnosis filed. The proposed CNN methods were tested on three datasets, including motor bearing dataset, self-priming centrifugal pump fault diagnosis dataset, and axial piston hydraulic pump fault diagnosis dataset, and they achieve the prediction accuracies of 99.79%, 99.481%, and 100%, respectively, which outperform other DL and traditional methods. These results show the good potential of the proposed CNN methods in the data-driven fault diagnosis field.

The limitations of the proposed method include the following aspects for real applications. First, the most common faults conditions are needed to be detected and can be represented in the dictionary list type. Otherwise, the faults which have not been learned would be misclassified to be the known ones. Second, the training process is very time consuming, and a GPU hardware is essential. Based on these limitations, the future research works can be conducted in the following ways. First, this method can be modified to find an unknown fault conditions. Second, the CNN-based transfer learning can be studied further to reduce the training time.

REFERENCES

- [1] X. Dai and Z. Gao, "From model, signal to knowledge: A data-driven perspective of fault detection and diagnosis," *IEEE Trans. Ind. Informat.*, vol. 9, no. 4, pp. 2226–2238, Nov. 2013.
- [2] Z. Gao, C. Cecati, and S. X. Ding, "A survey of fault diagnosis and fault-tolerant techniques-Part I: Fault diagnosis with model-based and signal-based approaches," *IEEE Trans. Ind. Electron.*, vol. 62, no. 6, pp. 3757–3767, Jun. 2015.
- [3] Z. Gao, C. Cecati, and S. X. Ding, "A survey of fault diagnosis and fault-tolerant techniques-Part I: Fault diagnosis with model-based and signal-based approaches," *IEEE Trans. Ind. Electron.*, vol. 62, no. 6, pp. 3757–3767, Jun. 2015.
- [4] D. Wang and W. T. Peter, "Prognostics of slurry pumps based on a moving-wear degradation index and a general sequential monte carlo method," *Mech. Syst. Signal Process.*, vol. 56, pp. 213–229, May 2015.
- [5] A. Gandomi and M. Haider, "Beyond the hype: Big data concepts, methods, and analytics," *Int. J. Inf. Manage.*, vol. 35, no. 2, pp. 137–144, Apr. 2015.
- [6] T. Aydmj and R. P. W. Duin, "Pump failure determination using support vector data description," in *Advances in Intelligent Data Analysis (Lecture Notes in Computer Science)*. Berlin, Germany: Springer, 1999, pp. 415–425.
- [7] D. Wijayasekara, O. Linda, M. Manic, and C. Rieger, "FN-DFE: Fuzzy-neural data fusion engine for enhanced resilient state-awareness of hybrid energy systems," *IEEE Trans. Cybern.*, vol. 44, no. 11, pp. 2065–2075, Nov. 2014.
- [8] Y. Shatnawi and M. Al-Khassaweneh, "Fault diagnosis in internal combustion engines using extension neural network," *IEEE Trans. Ind. Electron.*, vol. 61, no. 3, pp. 1434–1443, Mar. 2014.
- [9] D. You, X. Gao, and S. Katayama, "WPD-PCA-based laser welding process monitoring and defects diagnosis by using FNN and SVM," *IEEE Trans. Ind. Electron.*, vol. 62, no. 1, pp. 628–636, Jan. 2015.
- [10] J. Schmidhuber, "Deep learning in neural networks: An overview," *Neural Netw.*, vol. 61, pp. 85–117, Jan. 2015.
- [11] Y. LeCun, Y. Bengio, and G. Hinton, "Deep learning," *Nature*, vol. 521, no. 7553, pp. 436–444, May 2015.
- [12] H. Shao, H. Jiang, X. Zhang, and M. Niu, "Rolling bearing fault diagnosis using an optimization deep belief network," *Meas. Sci. Technol.*, vol. 26, no. 11, Sep. 2015, Art. no. 115002.
- [13] L. Wen, L. Gao, and X. Y. Li, "A new deep transfer learning based on sparse auto-encoder for fault diagnosis," *IEEE Trans. Syst., Man, Cybern., Syst.*, Oct. 2017, doi: 10.1109/TSMC.2017.2754287.
- [14] C. Lu, Z. Wang, W. Qin, and J. Ma, "Fault diagnosis of rotary machinery components using a stacked denoising autoencoder-based health state identification," *Signal Process.*, vol. 130, pp. 377–388, Jan. 2017.
- [15] H. Shao, H. Jiang, F. Wang, and H. Zhao, "An enhancement deep feature fusion method for rotating machinery fault diagnosis," *Knowl.-Based Syst.*, vol. 119, pp. 200–220, Mar. 2017.
- [16] Y. Lei, F. Jia, J. Lin, S. Xing, and S. X. Ding, "An intelligent fault diagnosis method using unsupervised feature learning towards mechanical big data," *IEEE Trans. Ind. Electron.*, vol. 63, no. 5, pp. 3137–3147, May 2016.
- [17] T. Ince, S. Kiranyaz, L. Eren, M. Askar, and M. Gabbouj, "Real-time motor fault detection by 1-D convolutional neural networks," *IEEE Trans. Ind. Electron.*, vol. 63, no. 11, pp. 7067–7075, Nov. 2016.
- [18] C. Lu, Y. Wang, M. Ragulskis, and Y. Cheng, "Fault diagnosis for rotating machinery: A method based on image processing," *PLoS One*, vol. 11, no. 10, Oct. 2016, Art. no. e0164111.
- [19] E. J. Henley, "Application of expert systems to fault diagnosis," in *Proc. AIChE Annu. Meeting*, San Francisco, CA, USA, 1984.
- [20] S. Yin, S. X. Ding, X. C. Xie, and H. Luo, "A review on basic data-driven approaches for industrial process monitoring," *IEEE Trans. Ind. Electron.*, vol. 61, no. 11, pp. 6418–6428, Nov. 2014.

- [21] S. Yin, H. Luo, and S. X. Ding, "Real-time implementation of fault-tolerant control systems with performance optimization," *IEEE Trans. Ind. Electron.*, vol. 61, no. 5, pp. 2402–2411, May 2014.
- [22] S. Yin, G. Wang, and H. Gao, "Data-driven process monitoring based on modified orthogonal projections to latent structures," *IEEE Trans. Control Syst. Technol.*, vol. 24, no. 4, pp. 1480–1487, Jul. 2016.
- [23] M. Grbovic, W. Li, N. A. Subrahmanya, A. K. Usadi, and S. Vucetic, "Cold start approach for data-driven fault detection," *IEEE Trans. Ind. Informat.*, vol. 9, no. 4, pp. 2264–2273, Nov. 2013.
- [24] R. Zhao, R. Yan, Z. Chen, K. Ma3o, Peng Wang, and R. X. Gao, "Deep learning and its applications to machine health monitoring: A survey," Dec. 2016. [Online]. Available: arXiv preprint arXiv:1612.07640
- [25] F. Jia, Y. Lei, J. Lin, X. Zhou, and N. Lu, "Deep neural networks: A promising tool for fault characteristic mining and intelligent diagnosis of rotating machinery with massive data," *Mech. Syst. Signal Process.*, vol. 72, pp. 303–315, May 2016.
- [26] L. Liao, W. Jin, and R. Pavel, "Enhanced restricted Boltzmann machine with prognosability regularization for prognostics and health assessment," *IEEE Trans. Ind. Electron.*, vol. 63, no. 11, pp. 7076–7083, Nov. 2016.
- [27] M. Gan and C. Wang, "Construction of hierarchical diagnosis network based on deep learning and its application in the fault pattern recognition of rolling element bearings," *Mech. Syst. Signal Process.*, vol. 72, pp. 92–104, May 2016.
- [28] H. C. Cho, J. Knowles, M. S. Fadali, and K. S. Lee, "Fault detection and isolation of induction motors using recurrent neural networks and dynamic Bayesian modeling," *IEEE Trans. Control Syst. Technol.*, vol. 18, no. 2, pp. 430–437, Mar. 2010.
- [29] O. Abdeljaber, O. Avcı, S. Kiranyaz, M. Gabbouj, and D. J. Inman, "Real-time vibration-based structural damage detection using one-dimensional convolutional neural networks," *J. Sound Vib.*, vol. 388, pp. 154–170, Feb. 2017.
- [30] X. Guo, L. Chen, and C. Shen, "Hierarchical adaptive deep convolution neural network and its application to bearing fault diagnosis," *Measurement*, vol. 93, pp. 490–502, Nov. 2016.
- [31] U. P. Chong, "Signal model-based fault detection and diagnosis for induction motors using features of vibration signal in two-dimension domain," *Strojnicki vestnik-J. Mech. Eng.*, vol. 57, no. 9, pp. 655–666, Sep. 2011.
- [32] M. Kang and J. M. Kim, "Reliable fault diagnosis of multiple induction motor defects using a 2-D representation of Shannon wavelets," *IEEE Trans. Magn.*, vol. 50, no. 10, pp. 1–13, Oct. 2014.
- [33] B. Li, P. L. Zhang, D. S. Liu, S. S. Mi, G. Q. Ren, and H. Tian, "Feature extraction for rolling element bearing fault diagnosis utilizing generalized S transform and two-dimensional non-negative matrix factorization," *J. Sound Vib.*, vol. 330, no. 10, pp. 2388–2399, May 2011.
- [34] B. A. Olshausen and D. J. Field, "Emergence of simple-cell receptive field properties by learning a sparse code for natural images," *Nature*, vol. 381, no. 6583, pp. 607–609, Jun. 1996.
- [35] Y. Bengio, A. Courville, and P. Vincent, "Representation learning: A review and new perspectives," *IEEE Trans. Pattern Anal. Mach. Intell.*, vol. 35, no. 8, pp. 1798–1828, Aug. 2013.
- [36] Y. LeCun, "LeNet-5, convolutional neural networks," 2015. [Online]. Available: <http://yann.lecun.com/exdb/lenet>. 2015
- [37] A. Krizhevsky, I. Sutskever, and G. E. Hinton, "Imagenet classification with deep convolutional neural networks," in *Proc. Adv. Neural Inf. Process. Syst.*, 2012, pp. 1097–1105.
- [38] K. Simonyan and A. Zisserman, "Very deep convolutional networks for large-scale image recognition," Sep. 2014. [Online]. Available: arXiv:1409.1556.
- [39] C. Szegedy *et al.*, "Going deeper with convolutions," in *Proc. IEEE Conf. Comput. Vis. Pattern Recognit.*, 2015, pp. 1–9.
- [40] S. Hong, Q. Wu, H. Xie, Y. Chen, and Y. Kou, "A novel coupled template for face recognition based on a convolutional neural network," in *Proc. IEEE 6th Int. Conf. Intell. Syst. Design Eng. Appl.*, Aug. 2015, pp. 52–56.
- [41] X. D. Ren, H. N. Guo, G. C. He, X. Xu, C. Di, and S. H. Li, "Convolutional neural network based on principal component analysis initialization for image classification," in *Proc. IEEE Int. Conf. Data Sci. Cyberspace*, Jun. 2016, pp. 329–334.
- [42] W. A. Smith and R. B. Randall, "Rolling element bearing diagnostics using the case western reserve university data: A benchmark study," *Mech. Syst. Signal Process.*, vol. 64, pp. 100–131, Dec. 2015.
- [43] X. Zhang, Y. Liang, and J. Zhou, "A novel bearing fault diagnosis model integrated permutation entropy, ensemble empirical mode decomposition and optimized SVM," *Measurement*, vol. 69, pp. 164–179, Jun. 2015.



Long Wen was born in Hubei, China, in December 1988. He received the B.E. and Ph.D. degrees in industrial engineering from the Huazhong University of Science and Technology (HUST), Wuhan, China, in 2010 and 2014, respectively.

He is currently a Postdoctor in the Department of Industrial and Manufacturing Systems Engineering, State Key Laboratory of Digital Manufacturing Equipment and Technology, School of Mechanical Science and Engineering, HUST.

His research interests include deep learning, machine learning, and intelligent algorithms.



Xinyu Li received the Ph.D. degree in industrial engineering from the Huazhong University of Science and Technology (HUST), Wuhan, China, in 2009.

He is currently an Associate Professor in the Department of Industrial and Manufacturing Systems Engineering, State Key Laboratory of Digital Manufacturing Equipment and Technology, School of Mechanical Science and Engineering, HUST. He had published more than 60 refereed papers. His research interests include

intelligent algorithms, big data, and machine learning.



Liang Gao (M'08) received the Ph.D. degree in mechatronic engineering from the Huazhong University of Science and Technology (HUST), Wuhan, China, in 2002.

He is currently a Professor in the Department of Industrial and Manufacturing System Engineering, State Key Laboratory of Digital Manufacturing Equipment and Technology, School of Mechanical Science and Engineering, HUST. He had published more than 140 refereed papers. His research interests include operations

research and optimization, big data, and machine learning.



Yuyan Zhang was born in Henan Province, China, in 1989. He received the B.S. degree in mechanical design, manufacturing and automation and the M.S. degree in mechatronic engineering from Xiangtan University, Xiangtan, China, in 2012 and 2015, respectively.

He is currently pursuing the Ph.D. degree in the department of industrial & manufacturing systems engineering at Huazhong University of Science and Technology, Wuhan, China. His research interests include deep learning and its

applications in intelligent fault diagnosis.